**REVIEW**

# Four-dimensional quantitative analysis using FDG-PET in clinical oncology

Nagara Tamaki[1] · Kenji Hirata[2] · Tomoya Kotani[1] · Yoshitomo Nakai[1] · Shigenori Matsushima[1] · Kei Yamada[1]

## Abstract

Positron emission tomography (PET) with F-18 fluorodeoxyglucose (FDG) has been commonly used in many oncological areas. High-resolution PET permits a three-dimensional analysis of FDG distributions on various lesions in vivo, which can be applied for tissue characterization, risk analysis, and treatment monitoring after chemoradiotherapy and immunotherapy. Metabolic changes can be assessed using the tumor absolute FDG uptake as standardized uptake value (SUV) and metabolic tumor volume (MTV). In addition, tumor heterogeneity assessment can potentially estimate tumor aggressiveness and resistance to chemoradiotherapy. Attempts have been made to quantify intratumoral heterogeneity using radiomics. Recent reports have indicated the clinical feasibility of a dynamic FDG PET-computed tomography (CT) in pilot cohort studies of oncological cases. Dynamic imaging permits the assessment of temporal changes in FDG uptake after administration, which is particularly useful for differentiating pathological from physiological uptakes with high diagnostic accuracy. In addition, several new parameters have been introduced for the in vivo quantitative analysis of FDG metabolic processes. Thus, a four-dimensional FDG PET-CT is available for precise tissue characterization of various lesions. This review introduces various new techniques for the quantitative analysis of FDG distribution and glucose metabolism using a four-dimensional FDG analysis with PET-CT. This elegant study reveals the important role of tissue characterization and treatment strategies in oncology.

**Keywords** PET · FDG · Quantitative analysis · Cancer · Dynamic whole-body imaging

✉ Nagara Tamaki
natamaki@koto.kpu-m.ac.jp

Kenji Hirata
khirata@med.hokudai.ac.jp

Tomoya Kotani
kotani@koto.kpu-m.ac.jp

Yoshitomo Nakai
y-nakai@koto.kpu-m.ac.jp

Shigenori Matsushima
matsu@koto.kpu-m.ac.jp

Kei Yamada
kyamada@koto.kpu-m.ac.jp

1 Department of Radiology, Graduate School of Medical Science, Kyoto Prefectural University of Medicine, Kyoto, Japan

2 Department of Diagnostic Imaging, Hokkaido University Graduate School of Medicine, Sapporo, Japan

## Introduction

Various imaging modalities have played important roles in the diagnosis, staging, and therapeutic monitoring of cancer. Positron emission tomography (PET) has recently been applied in several oncological areas. Compared to several other noninvasive imaging modalities, PET is characteristically unique for the in vivo quantitative assessment of tumor characteristics [1, 2]. The accumulation of F-18 fluorodeoxyglucose (FDG) may reflect tumor characteristics based on its metabolic activity, including the membrane glucose transporter protein and hexokinase enzyme. High imaging contrast enhances the detection of these characteristics in many types of cancer [3–5].

Quantitative assessment of FDG uptake can often be used for treatment monitoring after chemotherapy or chemoradiotherapy [6–8]. Numerous studies have considered biochemical changes assessed using FDG-PET as a sensitive marker compared with morphological changes estimated using computed tomography (CT) or magnetic resonance

imaging (MRI). In addition, patients with a complete metabolic response after therapy may show better disease-free survival and overall survival than those with any other responses [9–21]. Precise assessment of treatment response is required, mainly because of the rapid progress in new treatments for various cancers.

Whole-body PET imaging allows the accurate staging and restaging of various cancers before and after treatment, in combination with CT or MRI. Such three-dimensional (3-D) analysis of FDG distribution using a high-resolution PET system and appropriate software enables the provision of important quantitative parameters for tissue characterization and treatment strategy. On the other hand, FDG uptake is present in many physiological conditions. Therefore, it is often difficult to differentiate pathological from physiological FDG uptake in routine static PET studies [22–28].

With the recent advances in technology, serial dynamic imaging after FDG administration has become possible [29–31]. Such dynamic imaging provides temporal parameters for quantitative analysis of temporal changes in FDG accumulation. Such new imaging methods permit a 3-D spatial analysis of FDG distribution with high-resolution PET imaging, and temporal analysis of FDG uptake changes after administration. Thus, a four-dimensional (4-D) analysis of FDG distribution is now possible and may provide new and valuable information regarding tissue characterization,

malignant and benign lesion differentiation, and physiological tracer accumulation [32, 33] (Fig. 1).

This review introduces various new techniques for the quantitative analysis of FDG distribution and glucose metabolism with a 4-D FDG analysis using PET-CT. This elegant study highlights the important role of tissue characterization and treatment strategies in oncology.

## Quantitative parameters

### FDG uptake concentration

High-resolution and sensitive PET systems provide several quantitative parameters for FDG distribution and glucose metabolism in oncology. Standardized uptake value (SUV) is one of the most commonly used PET parameters for estimating FDG uptake. The SUV represents the radioactivity concentration in the lesion at a single time point. The SUV is simply the ratio of the activity concentration in the target tissue or lesion to the activity concentration in the whole body. The SUV can be calculated using the following formula: SUV = [tissue tracer activity concentration [Bq/mL]]/ ([injected dose [Bq]]/[body weight [g]]) [6–8]. When the injected tracer was homogeneously distributed throughout the body, the SUV was defined to be 1.



**Fig. 1** Serial whole-body FDG-PET images (3 min each) approximately 60 min after FDG administration in a patient with lung cancer with pulmonary metastatic lung cancers. High and persistent uptake in the lung cancer and liver metastasis was noted, whereas some uptake motion changes were observed in the ureter and small intestine
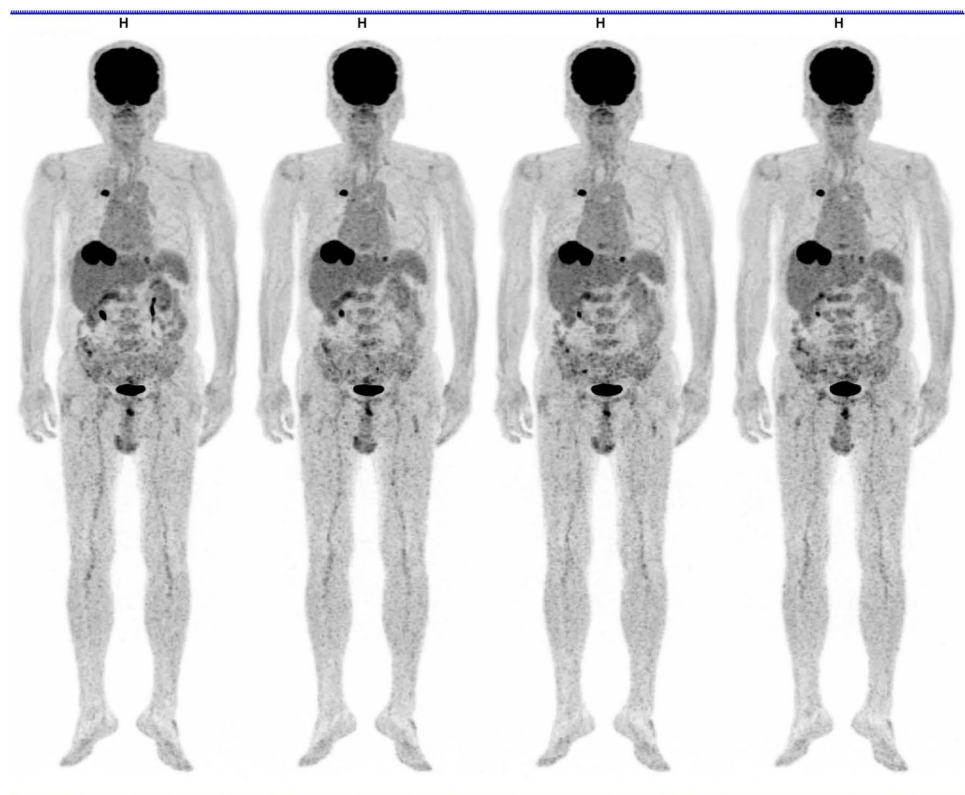
Metabolic changes are often assessed using the SUV value of the tumor. The SUV accounts for the differential partitioning of injected activity within the body. When the same PET camera and scan acquisition parameters are used, reasonable reproducibility of the SUV values can be achieved [34–36]. This SUV is commonly used in clinical oncological studies.

The maximal SUV (SUVmax) of a lesion is independent of the size of the region of interest (ROI). SUVmax is most commonly used in clinical practice because it is simple, reproducible, and readily available using widely used software [5, 34]. SUVmax and not SUVmean was used owing to metabolic heterogeneity or irregular tumor borders. However, the SUVmax is sensitive to image noise and motion. In addition, its value depends on the image quality of the PET/CT system. Notably, the state-of-art PET-CT scanners with high spatial resolution usually produce images with a high SUVmax. Such system-dependent values may cause difficulties in directly comparing various PET scanners' results.

The peak SUV (SUVpeak) was introduced to overcome the shortcomings of SUVmax as a hybrid of the mean value of radiotracer uptake within the ROI surrounding the highest-intensity voxel (generally $1 cm^3$ ROI surrounding the voxel with the highest activity). The SUVpeak is less susceptible to noise and scanner differences in spatial resolution. In addition, an index called SUL has been proposed [34], representing the standardized uptake value using the lean body mass index.

Accordingly, changes in SUVmax within the disease sites were used in one of the first iterations of the PET response criteria [37]. More recently, further refinements in the response criteria have been proposed. In particular, the PERCIST framework [34] has been widely adopted by the nuclear medicine community. Based on the same theoretical constructs as SUV measurement, variations in the analytical method have led to related parameters. These include SUL, representing SUV corrected for lean body mass rather than actual patient weight, and SUVpeak, which is the average of the most intense voxels within a relatively small volume of interest (VOI) [34]. SUVpeak was proposed within the PERCIST criteria and aimed to overcome the potential impact of isolated intense voxels on the results [38].

The patient's total weight is usually used to normalize the SUV. However, in obese people, SUV is overestimated in lesions and normal tissues because FDG is distributed mainly in non-fatty tissues, whereas the percentage of adipose tissue is high in obese people, with minimal FDG accumulation in the fat. The use of SUL rather than SUV normalization by total weight is recommended for obese patients.

## Volumetric measurement

PET/CT provides an opportunity to evaluate disease burden. The SUVmax metrics indicate the radioactivity concentration of a very small region within the tumor and, therefore, do not consider the tumor volume. At this point, PET differs from CT or MRI, where the tumor size is usually measured using a major axis. Indices for estimating tumor size have been established for PET. Among the various volumetric parameters of FDG PET, metabolic tumor volume (MTV) and total lesion glycolysis (TLG) are commonly used [39]. MTV represents the volume of the tumor with active FDG uptake (which is usually above a certain threshold, such as $SUV \geq 2.5$ or $SUV \geq 40\%$ SUVmax). TLG is calculated by multiplying the SUVmean of the total tumor by its MTV. Thus, TLG is the sum of the SUV within a lesion. These volumetric parameters have been used as prognostic indicators for various tumors, as described below.

## Heterogeneity measurement

Many malignant tumors tend to be naturally heterogeneous. Several mechanisms have been used to explain the heterogeneous nature of malignant tumors. First, tumors tend to develop from genetic mutations more frequently than normal cells, leading to heterogeneous biological behavior. Second, tumors grow rapidly, and develop a hypoxic region, resulting in elevated glucose consumption (Warburg effects) or severely decreased metabolism (necrosis). Third, tumor cells coexist with microenvironment cells, such as tumor-associated macrophages (TAM), cancer-associated fibroblasts (CAF), and myeloid-derived suppressor cells (MDSC). The variability of tumor proportions and activities may cause metabolic heterogeneity in cancer tissues as a whole. Generally, tumor heterogeneity may be associated with aggressiveness, growth speed, and metastatic potential, all of which are important for clinical management.

Tumor heterogeneity can be described qualitatively as 'homogeneous' or 'heterogeneous' (sometimes, 'inhomogeneous'). In radiology reports of FDG PET-CT, radiologists and nuclear medicine physicians often evaluate tumors using qualitative categories; however, such expressions are subjective and poorly reproducible. Especially, the criteria to distinguish 'homogeneous' from 'heterogeneous' are unclear. In addition, it is difficult to describe the degree of tumor heterogeneity.

In this context, radiomics has recently been introduced as a technique that uses a mathematical model to quantify heterogeneity by extracting numerical features from radiological images [40]. Individual features only represent image characteristics and are not immediately clinically useful. However, by combining several features and machine learning techniques, such as random forest and

support vector machine, some clinical information, such as tumor malignancy, treatment response, and survival, could be predicted.

The simplest radiometric method encloses the tumor and a region of interest (ROI) or volume of interest (VOI) if it is 3-D, creates a histogram of voxel values (usually, SUV) within the ROI/VOI, and calculates the mean, standard deviation, energy, entropy, kurtosis, and skewness. This is typically called a first-order statistic. This may represent tumor heterogeneity to some extent; however, this method does not consider spatial relationships. In other words, this method does not distinguish adjacent from distant voxels. Therefore, when researchers apply radiomics or texture analysis to their data, they usually employ higher-order statistics that can incorporate the spatial distribution of the voxels. To calculate higher-order features, it is necessary to calculate a matrix (that is, an intermediate product) that represents heterogeneity, such as the gray-level co-occurrence matrix (GLCM), gray-level size-zone matrix (GLSZM), gray-level run-length matrix (GLRLM), or neighborhood gray-tone difference matrix (NGTDM). Each matrix generates several features. The imaging biomarker standardization initiative (IBSI) described 174 radiomic features with clear definitions [41]. It may be difficult for beginners in this field to understand this large number of features simultaneously. Thus, here in this article, we would like to focus on the 'entropy calculated from GLCM' (EntropyGLCM), which is not only easy to understand but also clinically useful in esophageal and lung cancers [42]. In addition, EntropyGLCM is

relatively robust and less sensitive to variability in tumor boundary determination [42].

Figure 2 illustrates a case in which EntropyGLCM was calculated from an FDG PET image of a patient with a neck lesion of diffuse large B-cell lymphoma (Fig. 2a, arrow). The first step was to determine the tumor area. If the tumor boundary is determined manually, the reduced reproducibility of VOI reduces the reliability of the texture features. Thus, it is better to segment the tumor automatically. In this case, we delineated the tumor using an SUV of ≥ 3. The red area represents the segmented tumor region (Fig. 2d). All voxels within the region were extracted (Fig. 2e). It is important to record the (x, y, z) coordinates with the SUVs to preserve the locations of the voxels. In this example, 7206 voxels were extracted from the VOI.

The SUV is a continuous value and is often discretized for texture analysis. A common method is to discretize the SUV with a fixed number of bins between the SUVmin and SUVmax (in this example, SUVmin = 3.00, SUVmax = 22.45, and 64 bins). An alternative method is to fix the SUVmin and SUVmax at 0 and 20, respectively.

The GLCM was calculated from the discretized voxel list, which can be regarded as a correlation plot between adjacent voxels. Note that in the 3D space, there are 13 definitions of connected voxel directions whose distance is less than 2 voxels (that is, 1, $\sqrt{2}$ or $\sqrt{3}$); therefore, it is common to compute the GLCM in 13 different ways. For simplification, we focused on voxels adjacent to each other in the x-axis direction, such as (75, 65, 360), and (76, 65, 360). The
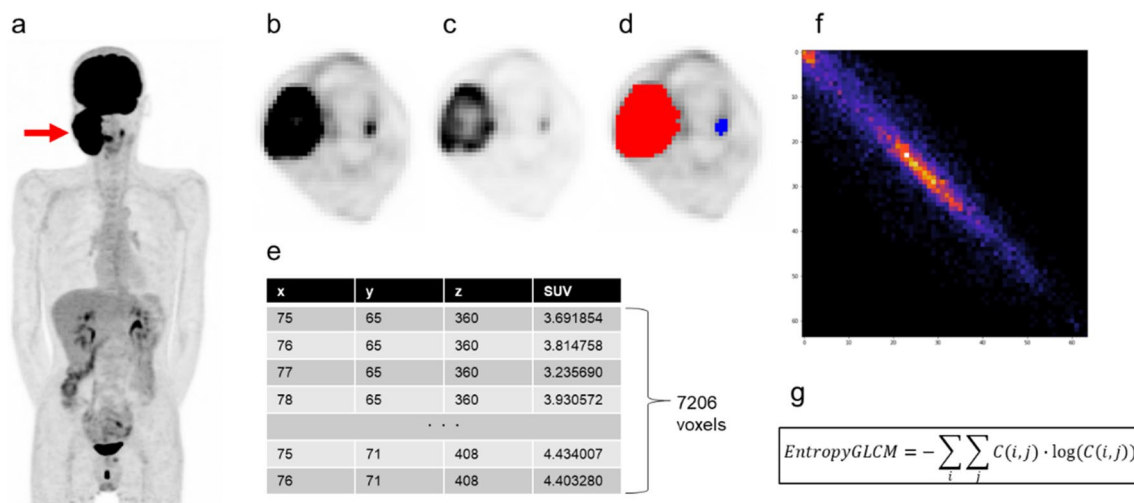


**Fig. 2** An example of the texture analysis procedure. **a** Maximum intensity projection of FDG-PET of a male patient in his 50 s with diffuse large B-cell lymphoma. A huge tumor in the right neck was shown (arrow). **b** A transaxial slice showing the tumor with SUV window 0 to 6 indicates that the entire tumor metabolizes homogenously; however **c** the same slice with SUV windows 0 to 15 depicts the intra-tumoral heterogeneity of metabolism. **d** The tumor was segmented using SUV≥3 as the criteria. **e** A total of 7206 voxels were extracted from the segmented region. Not only SUV but also the (x,y,z) coordinate are important for the following calculation. **f** After 64-degree discretization, the GLCM (64×64) was calculated. **g** EntropyGLCM was calculated from the GLCM. The value was 6.60 in this case

GLCM is shown as a scatter diagram (Fig. 2f). Note that if all voxel pairs have the same value, the scatter diagram will be the line of identity ($y = x$).

Finally, the EntropyGLCM was calculated using the following formula:

$$\text{Entropy } GLCM = -\sum_i \sum_j C(i,j) \cdot \log(C(i,j))$$

where C(i,j) is the GLCM probability value. As it is a 'probability' value, C (i, j) is normalized as follows:

$$\sum_i \sum_j C(i,j) = 1$$

Similar to the general definition, entropy is the negative of the inner product of the probability and log of the probability values. Entropy can be calculated using either a histogram or GLCM; therefore, it is important to note which one it represents. Different feature names, such as EntropyHist and EntropyGLCM, are commonly used for this purpose.

There are two popular free software tools for radiomics or texture feature calculation: *LIFEx* [43] and *PyRadiomics* [44]. *LIFEx* is an integrated environment with a graphical user interface (GUI). *PyRadiomics* is a python library package. If a GUI is needed for *PyRadiomics*, *3D Slicer* can work together.

Among several problems in radiomics, robustness, and replicability seem to be the largest [45]. Recently, ComBat harmonization was proposed to solve this problem [46, 47].

## Temporal measurement

While most of the FDG parameters are derived through static PET imaging, there are a few trials that assessed temporal changes in FDG distribution using dynamic PET studies. For instance, dual-time-point PET imaging, which obtains both early standard and delayed PET images, has been used to differentiate benign from malignant lesions [31–33]. In addition to these studies that used visual assessment, the retention index (percentage difference in SUV between early and delayed images) was calculated [48].

There are new strategies for the generation of parametric images (pixel-by-pixel analysis) based on graphical analysis, such as the Patlak method [49, 50]. The graphical analysis is simple, and robust, and enables the direct estimation of the primary kinetic macro-components of tracer uptake across multiple fields of view. Serial dynamic whole-body PET imaging is considered a suitable method for assessing temporal changes in tracer uptake. More recently, several reports have indicated the clinical feasibility of dynamic FDG PET-CT in a pilot cohort of oncological cases [51–53].

The Patlak model can be applied when the tracer reaches a steady state between blood and tissue. This model estimates the Patlak slope (Ki), which is the rate of irreversible uptake, and the Patlak intercept, which is the apparent distribution volume (DV), of the nonmetabolized tracer (Fig. 3). Accordingly, the metabolic rate of FDG was estimated as follows: Metabolic rate of FDG (MRFDG) = Ki × blood glucose [49, 50].

A preliminary study indicated that multi-pass whole-body PET Ki parametric imaging that utilizes robust Patlak graphical analysis may achieve equivalent or potentially, superior lesion detectability than standard-of-care



**Fig. 3** Patlak analysis concept. Ki image and DV image can be obtained from this analysis
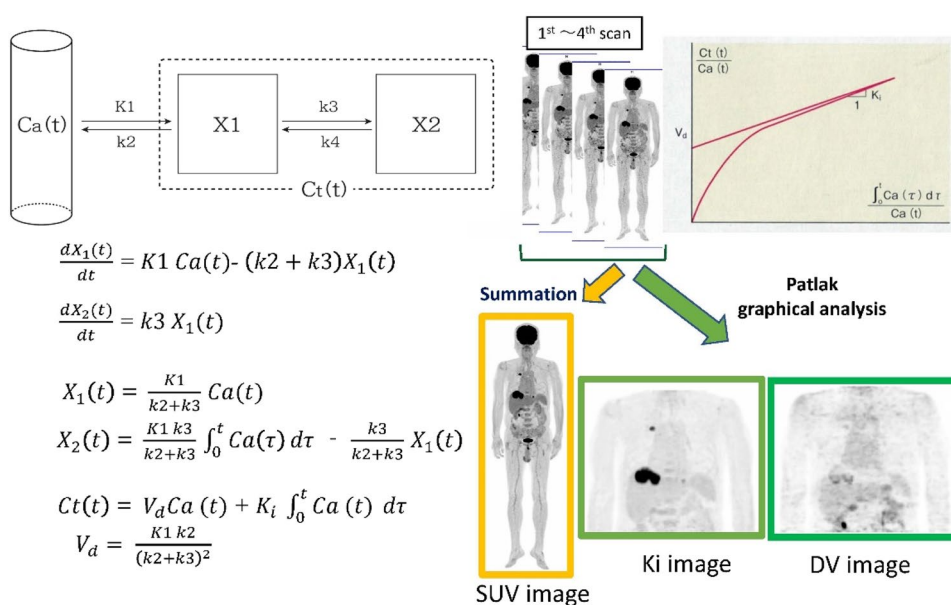
SUV imaging with reduced false-positive rates in routine oncology applications [52]. Ki parametric imaging seems to be particularly valuable for differentiating abnormal lesion uptake with a gradual increase in FDG uptake from physiological uptake areas and a gradual decrease in uptakes, such as in the liver and blood vessels. Ki may reflect count changes; therefore, it has the potential to enhance the detection of abnormal FDG uptake lesions in high background areas [53, 54].

A key issue in the kinetic analysis is obtaining a suitable input function for graphical analysis. Arterial or arterialized venous blood sampling is commonly performed, particularly for brain studies; however, this method is apparently invasive [55–58]. An image-based input function can be obtained using serial dynamic PET imaging, which covers large arterial blood regions such as the left ventricle and aorta [59]. Such a precise FDG kinetic analysis seems rather complicated and remains under investigation. Recently, a standardized input function has been proposed as a surrogate that may facilitate such parametric studies compared to the actual measurement of the input function on rapid dynamic imaging in cardiac areas [60–63]. Serial dynamic FDG-PET imaging using either actual early dynamic imaging or a standardized input function may hold new promise for quantitative analysis of glucose metabolism for pre-vise tissue characterization in a variety of fields, including oncology.

Table 1 summarizes the advantages and disadvantages of each quantitative parameter on 3-D and 4-D PET analyses. While the SUV parameter is commonly used, the 3D PET analysis permits the estimation of the number of volumetric and distribution parameters. New and valuable information regarding metabolic parameters is provided by 4-D analysis. However, such parameters require dynamic acquisition; thus, some difficulties remain in routine clinical settings.

## Clinical applications

These quantitative parameters have several clinical applications in clinical oncology. The 3-D quantitative analysis of FDG distribution provides important information for treatment strategies in oncology.

### Risk analysis

Quantitative analyses of FDG uptake have been performed for prognostic studies in patients with lung cancer. The SUV has been used for assessing either the likelihood of malignancy or aggressiveness in lung masses and as a result, the prognosis of known lung cancer has been assessed in many studies [9–17]. For instance, an earlier meta-analysis of 13 such studies evaluated the use of SUV for prognostic stratification of non-small cell lung cancers (NSCLCs) [9]. Several recent reports have suggested SUV analytical values for predicting patient outcomes in lung cancer [10–17]. A similar quantitative analysis of FDG uptake has also been applied in prognostic studies of other cancers [18–21].

Similar to SUV evaluation, volumetric analysis has been used as a prognostic biomarker. Despite the lack of a standardized method for its determination and its significant variability with different thresholds, MTV has a great potential for risk analysis in lung cancer [64, 65]. Moreover, tumor heterogeneity may have the potential for predicting tumor outcomes [66–68]. Heterogenic tumors may contain hypoxic cells that are resistant to chemoradiotherapy [69, 70]. Several PET radiopharmaceuticals are used to identify tumor hypoxia [71–74]. However, FDG, the most commonly used PET radiopharmaceutical, can potentially detect the presence of hypoxia based on heterogeneity distribution.

Radiomics, such as texture analysis, has the potential for semiquantitative analysis of spatial FDG distribution. The heterogeneity of FDG distribution has been used for risk analysis in various cancers [39, 75–77]. Recent reports

**Table 1** Various quantitative FDG parameters on 3-D and 4-D PET analysis

| Parameters | Estimation | Clinical advantages | Disadvantages |
|---|---|---|---|
| SUV | Uptake concentration (max, peak, or mean) | Well established | Only pixel uptake |
| MTV | Uptake volume | Prognostic value | Depend on threshold |
| TLG | Uptake volume × mean uptake | Prognostic value | Depend on threshold |
| Heterogeneity | Radiomic analysis (texture analysis etc.) | Treatment resistance | Sensitive to scanner performance and analysis method |
| Ki | Uptake slope (Patlak plot) | Metabolic parameter | Difficult to estimate Dynamic acquisition |
| DV | Distribution volume (Patlak plot) | ? | Difficult to estimate Dynamic acquisition |

*SUV* standardized uptake value, *MTV* metabolic tumor volume, *TLG* total lesion glycolysis

indicated that the heterogeneity of FDG uptake plays a key role in assessing lesion resistance against various treatments; therefore, the prognostic index uses various radiomics, including texture analysis [39]. Tumor heterogeneity is associated with tumor aggressiveness. Most tumors may have necrotic and hypoxic areas, which may indicate resistance to chemo-radiotherapy. Several recent reports considered such tumor heterogeneity assessed using FDG-PET as a prognostic marker in patients treated with chemoradiotherapy [78–82]. There is no gold standard method for estimating tumor heterogeneity using PET. In addition, suitable chemoradiotherapy has not yet been established for heterogeneous tumors. More clinical studies are needed to establish suitable image analysis and clinical management in these patients.

## Treatment response

As FDG uptake is more sensitive to changes induced by treatments rather than morphological analysis, changes in SUV are considered fundamental components of molecular imaging response criteria. Accordingly, SUV measurements are commonly applied in multicenter trials in oncological treatment studies [34, 37].

The assessment of treatment response using FDG PET-CT plays an important role in optimizing subsequent treatment strategies and predicting patient outcomes. Qualitative evaluation remains the most commonly used approach in clinical practice and quantitative assessment of FDG uptake has been applied for treatment monitoring in most malignancies. Recent reports and review articles evaluated the prognostic values of changes in FDG uptake (SUV change) in various cancers [19, 83–89]. In a recent study involving nine PET/CT scanners across six institutions, quantitative SUV analysis demonstrated the ability of FDG PET-CT to predict 12-month overall survival from immune checkpoint inhibitor therapy using the EORTC, PERCIST, and imPERCIST criteria [90, 91].

Diffuse large B-cell lymphoma (DLBCL) and Hodgkin lymphoma have been the most extensively studied cancers for risk stratification and outcomes using FDG PET/CT. Interim PET performed after two or four cycles of chemotherapy has been proposed as a tool for adapting therapy in patients with good responses [92, 93]. In addition, therapy modification or a more aggressive therapy may be required in patients with progressive disease. High-risk patients are not accurately identified by the current prognostic scoring systems [87]. Qualitative PET analysis using the Deauville criteria, as previously described, has been used for the accurate analysis of treatment effects and outcomes [94, 95]. The prognostic role of quantitative PET parameters, particularly MTV, has been demonstrated in many lymphoma subtypes, including DLBCL [95–98]. Patients with a high disease burden, estimated using the MTV, are at a higher risk of treatment failure and a shorter survival rate.

## Use of temporal change

The assessment of temporal changes in FDG uptake using dynamic imaging has several clinical advantages over static imaging. Serial assessment of changes in FDG uptake, even within a short period, is useful for distinguishing pathological from physiological uptake, especially in the abdominal regions [32, 33, 99]. In the dynamic image evaluation, physiologically changed uptake was frequently found in the gastrointestinal regions and ureters. On the other hand, most benign and malignant lesions showed no visual change in serial images, suggesting the need for a high diagnostic value for differentiating physiological FDG uptake from pathological FDG uptake based on the presence of uptake changes on serial dynamic imaging. These dynamic PET studies may minimize the need for delayed PET imaging [33].

In addition, most malignant lesions may show a gradual increase in FDG uptake, indicating high glucose (or FDG) metabolism, as compared to minimal change or decrease in benign lesions and physiological uptake areas. Recent reports indicated that the target-to-background ratio of Ki in the Patlak analysis was higher than the commonly used SUV values, indicating a higher contrast on the parametric PET images than on the static images [53, 54, 99–101] (Fig. 4). Some of these preliminary studies did not show significant differences in the contrast between malignant and benign lesions. However, Ki, a marker of FDG metabolism, seems to be more suitable for predicting tumor cellular function and aggressiveness than SUV, a static FDG uptake marker in lung and breast cancer [97–105]. As many PET centers have had the chance to apply their up-to-date technology for parametric FDG analysis, these preliminary results will be confirmed in many oncology areas.

PET has significant advantages in the quantitative analysis of tracer activity distributions. In particular, 4-D PET analysis provides new metabolic parameters. A more precise assessment of the clinical values of such parametric imaging is expected in oncology with more patient-based studies in the future.

## Future perspectives

In addition to the introduction of elegant data analyses, instrumental developments have been conducted.

PET-CT systems equipped with silicon photomultiplier–based detectors (digital PET) have been introduced. This new system has improved detection capabilities that might contribute to enhanced diagnostic performance and reduce the activity administration or scan duration. In

**Fig. 4** Whole-body (top) images of SUV, Ki, and distribution volume (DV) parameters estimated from the serial dynamic imaging as shown in Fig. 1. Axial images of the SUV and Ki are shown at the bottom. Higher contrast of the lesions was noted with attenuated physiologic uptake in the mediastinum and liver on Ki images
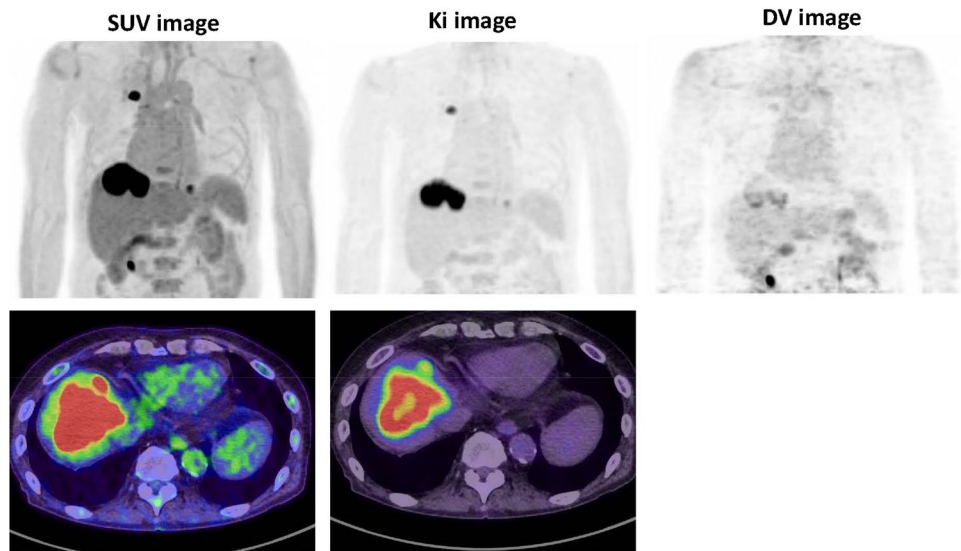


addition, quantitative capability has been improved significantly owing to a higher spatial resolution and lesser scatter noise [106–108]. Such high performance of the PET system permits short and serial dynamic imaging with high-quality images. Thus, a better quantitative 4-D analysis of FDG PET/CT may be available in clinical oncology [54].

Such digital PET with their magnetic-susceptibility tolerance makes them ideal devices for use in PET-MR systems [109, 110]. There are many advantages of the combined analysis of PET and MRI in the clinical oncology field, which have been fully presented elsewhere [111, 112].

## Conclusion

FDG PET-CT can provide valuable clinical information regarding tumor metabolism and aggressiveness in various types of cancers. Various quantitative approaches have been introduced for image-based precision medicine, including tracer concentration, volume, and heterogeneity analysis using 3-D FDG distribution. Recent progress in PET imaging permits the temporal assessment of FDG uptake. Thus, a 4-D analysis of FDG PET-CT is available for the precise tissue characterization of various lesions. Such elegant studies will provide new and valuable information for tissue characterization and treatment strategies in oncology.

## Declarations

## References

1. Juweid ME, Cheson BD. Positron-emission tomography and assessment of cancer therapy. N Engl J Med. 2006;354:496–507.
2. Weber WA. Positron emission tomography as an imaging biomarker. J Clin Oncol. 2006;24:3282–92.
3. Fletcher JW, Djulbegovic B, Soares HP, Siegel BA, Lowe VJ, Lyman GH, Coleman RE, Wahl R, Paschold JC, Avril N, Einhorn LH, Suh WW, Samson D, Delbeke D, Gorman M, Shields AF. Recommendations on the use of ^{18}F-FDG PET in oncology. J Nucl Med. 2008;49:480–508.
4. El-Galaly TC, Gormsen LC, Hutchings M. PET/CT for staging: past, present, and future. Semin Nucl Med. 2017;48:4–16.
5. Fletcher JW, Djulbegovic B, Soares HP, Siegel BA, Lowe VJ, Lyman GH, Coleman RE, Wahl R, Paschold JC, Avril N, Einhorn LH, Suh WW, Samson D, Delbeke D, Gorman M, Shields AF. Recommendations on the use of ^{18}F-FDG PET in oncology. J Nucl Med. 2008;49(3):480–508.
6. Keyes JW Jr. SUV: standard uptake or silly useless value? J Nucl Med. 1995;36:1836–9.
7. Thie JA. Understanding the standardized uptake value, its methods, and implications for usage. J Nucl Med. 2004;45:1431–4.

8. Boellaard R, Krak NC, Hoekstra OS, Lammertsma AA. Effects of noise, image resolution, and ROI definition on the accuracy of standard uptake values: a simulation study. J Nucl Med. 2004;45:1519–27.

9. Berghmans T, Dusart M, Paesmans M, et al. Primary tumor standardized uptake value (SUVmax) measured on fluorodeoxyglucose positron emission tomography (FDG-PET) is of prognostic value for survival in non-small cell lung cancer (NSCLC): a systematic review and meta-analysis (MA) by the European Lung Cancer Working Party for the IASLC Lung Cancer Staging Project. J Thorac Oncol. 2008;3:6–12.

10. Wainer Z, Daniels MG, Callahan J, et al. Sex and SUVmax: sex-dependent prognostication in early non-small cell lung cancer. J Nucl Med. 2012;53:1676–85.

11. Chen HH, Chiu NT, Su WC, et al. Prognostic value of whole-body total lesion glycolysis at pretreatment FDG PET/CT in non-small cell lung cancer. Radiology. 2012;264:559–66.

12. Lasnon C, Desmonts C, Quak E, et al. Harmonizing SUVs in multicenter trials when using different generation PET systems: Prospective validation in non-small cell lung cancer patients. Eur J Nucl Med Mol Imaging. 2013;40:985–96.

13. Quak E, Le Roux PY, Hofman MS, et al. Harmonizing FDG PET quantification while maintaining optimal lesion detection: Prospective multicenter validation in 517 oncology patients. Eur J Nucl Med Mol Imaging. 2015;42:2072–82.

14. Qiu X, Liang H, Zhong W, et al. Prognostic impact of maximum standardized uptake value on ^{18}F-FDG PET/CT imaging of the primary lung lesion on survival in advanced non-small cell lung cancer: a retrospective study. Thorac Cancer. 2021;12:845–53.

15. Steiger S, Arvanitakis M, Sick B, et al. Analysis of prognostic values of various PET metrics in preoperative ^{18}F-FDG PET for early-stage bronchial carcinoma for progression-free and overall survival: significantly increased glycolysis is a predictive factor. J Nucl Med. 2017;58:1925–30.

16. Kasahara N, Kaira K, Yamaguchi K, et al. Fluorodeoxyglucose uptake is associated with low tumor-infiltrating lymphocyte levels in patients with small cell lung cancer. Lung Cancer. 2019;134:180–6.

17. Zhuang M, García DV, Kramer GM, et al. Variability and repeatability of quantitative uptake metrics in ^{18}F-FDG PET/CT of non-small cell lung cancer: Impact of segmentation method, uptake interval, and reconstruction protocol. J Nucl Med. 2019;60:600–7.

18. Joo I, Lee JM, Lee DH, Lee ES, Paeng JC, Lee SJ, Jang JY, Kim SW, Ryu JK, Lee KB. Preoperative Assessment of pancreatic cancer with FDG PET/MR imaging versus FDG PET/CT plus contrast-enhanced multidetector CT: a prospective preliminary study. Radiology. 2017;282(1):149–59.

19. Bonomo P, Merlotti A, Olmetto E, Bianchi A, Desideri I, Bacigalupo A, Franco P, Franzese C, Orlandi E, Livi L, Caini S. What is the prognostic impact of FDG PET in locally advanced head and neck squamous cell carcinoma treated with concomitant chemoradiotherapy? A systematic review and meta-analysis. Eur J Nucl Med Mol Imaging. 2018;45(12):2122–38.

20. Yi HK, Park YJ, Bae JH, Lee JK, Lee KH, Choi SH, Lee KH, Kim BT, Choi JY. Inverse prognostic relationships of ^{18}F-FDG PET/CT metabolic parameters in patients with distal bile duct cancer undergoing curative surgery. Nucl Med Mol Imaging. 2018;52(5):334–41.

21. Farina A, Gasperini C, Aparisi Gómez MP, Bazzocchi A, Fanti S, Nanni C. The role of FDG-PET and whole-body MRI in high grade bone sarcomas with particular focus on osteosarcoma. Semin Nucl Med. 2022;52(5):635–46.

22. Davidson T, Komisar O, Korach J, Felder S, Apter S, Ben-Haim S, Perri T. Physiologic uptake of ^{18}F-FDG in transposed ovaries may mimic metastasis on ^{18}F-FDG PET/CT imaging. Nucl Med Commun. 2018;39(2):171–8.

23. Parida GK, Roy SG, Kumar R. FDG-PET/CT in skeletal muscle: pitfalls and pathologies. Semin Nucl Med. 2017;47(4):362–72.

24. Rosenbaum SJ, Lind T, Antoch G, Bockisch A. False-positive FDG PET uptake–the role of PET/CT. Eur Radiol. 2006;16(5):1054–65.

25. Lakhani A, Khan SR, Bharwani N, Stewart V, Rockall AG, Khan S, Barwick TD. FDG PET/CT pitfalls in gynecologic and genitourinary oncologic imaging. Radiographics. 2017;37(2):577–94.

26. Sena Y, Matsumoto S, Silman C, Otsuka K, Kiyota T. Physiological ^{18}F-FDG uptake in the normal adult anal canal: evaluation by PET/CT. Ann Nucl Med. 2020;34(8):538–44.

27. Lee N, IeR Y, Park SY, Yoon H, Lee Y, Oh JK. Significance of incidental nasopharyngeal uptake on ^{18}F-FDG PET/CT: patterns of benign/physiologic uptake and differentiation from malignancy. Nucl Med Mol Imaging. 2015;49(1):11–8.

28. Nakamura S, Okochi K, Murata Y, Shibuya H, Kurabayashi T. [^{18}F]Fluorodeoxyglucose-PET/CT differentiation between physiological and pathological accumulations in head and neck. Nucl Med Commun. 2009;30(7):498–503.

29. Dahlbom M, Reed J, Young J. Implementation of true continuous bed motion in 2-D and 3-D whole-body PET scanning. IEEE Trans Nucl Sci. 2001;48(4):1465–9.

30. Osborne DR, Acuff S, Cruise S, Syed M, Neveu M, Stuckey A, Bradley Y. Quantitative and qualitative comparison of continuous bed motion and traditional step and shoot PET/CT. Am J Nucl Med Mol Imaging. 2014;5(1):56–64.

31. Rahmim A, Lodge MA, Karakatsanis NA, Panin VY, Zhou Y, McMillan A, Cho S, Zaidi H, Casey ME. Wahl RL Dynamic whole-body PET imaging: principles, potentials and applications. Eur J Nucl Med Mol Imag. 2019;46:501–18.

32. Nishimura M, Tamaki N, Matsushima S, Kiba M, Kotani T, Bamba C, Nakamura Y, Yamada K. Dynamic whole-body ^{18}F-FDG PET for differentiating abnormal lesions from physiological uptake. Eur J Nucl Med Mol Imaging. 2020;47(10):2293–300.

33. Kotani T, Nishimura M, Tamaki N, Matsushima S, Akiyama S, Kanayama T, Bamba C, Tanada Y, Nii T, Yamada K. Comparison between dynamic whole-body FDG-PET and early-delayed imaging for the assessment of motion in focal uptake in colorectal area. Ann Nucl Med. 2021;35(12):1305–11.

34. Wahl RL, Jacene H, Kasamon Y, et al. From RECIST to PERCIST: evolving considerations for PET response criteria in solid tumors. J Nucl Med. 2009;50(Suppl 1):122S-150S.

35. Weber WA, Ziegler SI, Thodtmann R, et al. Reproducibility of metabolic measurements in malignant tumors using FDG PET. J Nucl Med. 1999;40:1771–7.

36. Mhlanga JC, Durand D, Tsai HL, Durand CM, Leal JP, Wang H, Moore R, Wahl RL. Differentiation of HIV-associated lymphoma from HIV-associated reactive adenopathy using quantitative FDG PET and symmetry. Eur J Nucl Med Mol Imaging. 2014;41(4):596–604.

37. Young H, Baum R, Cremerius U, et al. Measurement of clinical and subclinical tumour response using [^{18}F]-fluorodeoxyglucose and positron emission tomography: review and 1999 EORTC recommendations. European organization for research and treatment of cancer (EORTC) PET study group. Eur J Cancer. 1999;35:1773–82.

38. Kramer GM, Frings V, Hoetjes N, Hoekstra OS, Smit EF, de Langen AJ, Boellaard R. Repeatability of quantitative whole-body ^{18}F-FDG PET/CT uptake measures as function of uptake interval and lesion selection in non-small cell lung cancer patients. J Nucl Med. 2016;57(9):1343–9.

39. Hirata K, Tamaki N. Quantitative FDG PET assessment for oncology therapy. Cancers (Basel). 2021;3(4):869.

40. Gillies RJ, Kinahan PE, Hricak H. Radiomics: Images are more than pictures, they are data. Radiology. 2016;278(2):563–77.

41. Zwanenburg A, Vallieres M, Abdalah MA, et al. The Image biomarker standardization initiative: Standardized quantitative radiomics for high-throughput image-based phenotyping. Radiology. 2020;295(2):328–38.

42. Orlhac F, Nioche C, Soussan M, Buvat I. Understanding changes in tumor texture indices in PET: A comparison between visual assessment and index values in simulated and patient data. J Nucl Med. 2017;5883:387–92.

43. Nioche C, Orlhac F, Boughdad S, Reuze S, Goya-Outi J, Robert C, Pellot-Barakat C, Soussan M, Frouin F, Buvat I. LIFEx: A freeware for radiomic feature calculation in multimodality imaging to accelerate advances in the characterization of tumor heterogeneity. Cancer Res. 2018;78(1):4786–9.

44. Van Griethuysen JJM, Fedorov A, Parmar C, Hosny A, Aucoin N, Narayan V, Beets-Tan RGH, Fillion-Robin JC, Pieper S, Aerrts HJW. Computational radiomics system to decode the radiographic phenotype. Cancer Res. 2017;77(21):e104–7.

45. Pineiro-Fiel M, Moscoso A, Pubul V, Ruibal A, Silva-Rodriguez J, Aguiar P. A systematic review of PET textural analysis and radiomics in cancer. Diagnostics (Basel). 2021;11(2):380.

46. Orlhac F, Boughdad S, Philippe C, Stalla-Bourdillon H, Nioche C, Champion L, Soussan M, Frouin F, Froiin V, Buvat I. A postreconstruction harmonization method for multicenter radiomic studies in PET. J Nucl Med. 2018;59(8):1321–8.

47. Orlhac F, Eertink J, Cottereau AS, Zijlstra J, Thieblemont C, Meignan M, Boellaard R, Buvat I. A guide to ComBat harmonization of imaging biomarkers in multicenter studies. J Nucl Med. 2022;63(2):172–9.

48. Rogasch JM, Steffen IG, Riedel S, Apostolova I, Wertzel H, Achenbach HJ, Steinkrüger FL, Kalinski T, Schultz M, Schreiber J, Amthauer H, Furth C. Dual time point imaging for F18-FDG-PET/CT does not improve the accuracy of nodal staging in non-small cell lung cancer patients. Eur Radiol. 2016;26(8):2808–18.

49. Patlak CS, Blasberg RG, Fenstermacher JD. Graphical evaluation of blood-to-brain transfer constants from multiple-time uptake data. J Cereb Blood Flow Metab. 1983;3:1–7.

50. Patlak CS, Blasberg RG. Graphical evaluation of blood-tobrain transfer constants from multiple-time uptake data. Generalizations J Cereb Blood Flow Metab. 1985;5:584–90.

51. Karakatsanis NA, Lodge MA, Tahari AK, Zhou Y, Wahl RL, Rahmim A. Dynamic whole-body PET parametric imaging: I Concept, acquisition protocol optimization and clinical application. Phys Med Biol. 2013;58:7391–418.

52. Karakatsanis NA, Lodge MA, Zhou Y, Wahl RL, Rahmim A. Dynamic whole-body PET parametric imaging: II. Task-Orient Statist Estimat Phys Med Biol. 2013;58:7419–45.

53. Fahmi G, Karakatsanis NA, Domenicantonio Di, Garibotto V, Zaidi H. Does whole-body Patlak $^{18}$F-FDG PET imaging improve lesion detectability in clinical oncology? Eur Radiol. 2019;29:4812–21.

54. Dias AH, Pedersen MF, Danielsen H, Munk OL, Gormsen LC. Clinical feasibility and impact of fully automated multiparametric PET imaging using direct Patlak reconstruction: evaluation of 103 dynamic whole-body $^{18}$F-FDG PET/CT scans. Eur J Nucl Med Mol Imaging. 2021;48:837–50.

55. Wang G, Qi J. Acceleration of the direct reconstruction of linear parametric images using nested algorithms. Phys Med Biol. 2010;55:1505–17.

56. Karakatsanis NA, Zhou Y, Lodge MA, Casey ME, Wahl RL, Zaidi H, et al. Generalized whole-body Patlak parametric imaging for enhanced quantification in clinical PET. Phys Med Biol. 2015;60:8643–73.

57. van der Weerdt AP, Klein LJ, Visser CA, Visser FC, Lammertsma AA. Use of arterialised venous instead of arterial blood for measurement of myocardial glucose metabolism during euglycaemic-hyperinsulinaemic clamping. Eur J Nucl Med Mol Imaging. 2002;29:663–9.

58. Chen K, Bandy D, Reiman E, Huang SC, Lawson M, Feng D, et al. Noninvasive quantification of the cerebral metabolic rate for glucose using positron emission tomography, $^{18}$F-fluoro-2-deoxyglucose, the Patlak method, and an image derived input function. J Cereb Blood Flow Metab. 1998;18:716–23.

59. van der Weerdt AP, Klein LJ, Boellaard R, Visser CA, Visser FC, Lammertsma AA. Image-derived input functions for determination of MRGlu in cardiac (18)F-FDG PET scans. J Nucl Med. 2001;42:1622–9.

60. Takikawa S, Dhawan V, Spetsieris P, Robeson W, Chaly T, Dahl R, et al. Noninvasive quantitative fluorodeoxyglucose PET studies with an estimated input function derived from a population-based arterial blood curve. Radiology. 1993;188:131–6.

61. Shiozaki T, Sadato N, Senda M, Ishii K, Tsuchida T, Yonekura Y, et al. Noninvasive estimation of FDG input function for quantification of cerebral metabolic rate of glucose: optimization and multicenter evaluation. J Nucl Med. 2000;41:1612–8.

62. Vriens D, de Geus-Oei LF, Oyen WJ, Visser EP. A curve-fitting approach to estimate the arterial plasma input function for the assessment of glucose metabolic rate and response to treatment. J Nucl Med. 2009;50:1933–9.

63. Naganawa M, Gallezot JD, Shah V, Mulnix T, Young C, Dias M, Chen MK, Smith AM, Carson RE. Assessment of population-based input functions for Patlak imaging of whole body dynamic $^{18}$F-FDG PET. EJNMMI Physics. 2020;7:67.

64. Dall'Olio FG, Calabro D, Conci N, et al. Baseline total metabolic tumour volume on 2-deoxy-2-[$^{18}$F]fluoro-d-glucose positron emission tomography-computed tomography as a promising biomarker in patients with advanced non-small cell lung cancer treated with first-line pembrolizumab. Eur J Cancer. 2021;150:99–107.

65. Kolinger GD, Vallez García D, Kramer GM, et al. Repeatability of [$^{18}$F] FDG PET/CT total metabolic active tumour volume and total tumour burden in NSCLC patients. EJNMMI Res. 2019;9:14.

66. Karahan Şen NP, Alataş Ö, Gülcü A, Özdoğan Ö, Derebek E, Çapa KG. The role of volumetric and textural analysis of pretreatment $^{18}$F-fluorodeoxyglucose PET/computerized tomography images in predicting complete response to transarterial radioembolization in hepatocellular cancer. Nucl Med Commun. 2022;43(7):807–14.

67. Mikhaeel NG, Heymans MW, Eertink JJ, de Vet HCW, Boellaard R, Dührsen U, Ceriani L, Schmitz C, Wiegers SE, Hüttmann A, Lugtenburg PJ, Zucca E, Zwezerijnen GJC, Hoekstra OS, Zijlstra JM, Barrington SF. Proposed new dynamic prognostic index for diffuse large B-cell lymphoma: international metabolic prognostic index. J Clin Oncol. 2022;40(21):2352–60.

68. Bouron C, Mathie C, Seegers V, Morel O, Jézéquel P, Lasla H, Guilleminet C, Girault S, Lacombe M, Sher A, Lacoeuille F, Patsouris A, Testard A. Prognostic value of metabolic, volumetric and textural parameters of baseline [ 18F]FDG PET/CT in early triple-negative breast cancer. Cancers (Basel). 2022;14(3):637.

69. Jubb AM, Buffa FM, Harris AL. Assessment of tumour hypoxia for prediction of response to therapy and cancer prognosis. J Cell Mol Med. 2010;14:18–29.

70. Harrison L, Blackwell K. Hypoxia and anemia: factors in decreased sensitivity to radiation therapy and chemotherapy? Oncologist. 2004;9(Suppl 5):31–40.

71. Lewis JS, Sharp TL, Laforest R, Fujibayashi Y, Welch MJ. Tumor uptake of

copper-diacetyl-bis(N(4)-methylthiosemicarbazone): effect of changes in tissue oxygenation. J Nucl Med. 2001;42:655–61.

72. O'Donoghue JA, Zanzonico P, Pugachev A, Wen B, Smith-Jones P. Cai S et al Assessment of regional tumor hypoxia using ^{18}F-fluoromisonidazole and [64]Cu(II)-diacetyl-bis(N4-methylthiosemicarbazone) positron emission tomography: comparative study featuring microPET imaging, $Po_2$ probe measurement, autoradiography, and fluorescent microscopy in the R3327-AT and FaDu rat tumor models. Int J Radiat Oncol Biol Phys. 2005;61:1493–502.

73. Fatema CN, Zhao S, Zhao Y, Yu W, Nishijima K, Yasuda K, et al. Dual tracer evaluation of dynamic changes in intratumoral hypoxic and proliferative states after radiotherapy of human head and neck cancer xenografts using radiolabeled FMISO and FLT. BMC Cancer. 2014;14:692.

74. Tamaki N, Hirata K. Tumor hypoxia: a new PET imaging biomarker in clinical oncology. Int J Clinical Oncol. 2016;21:619–25.

75. Chitalia R, Viswanath V, Pantel A, Peterson LM, Gastounioti A, Cohen EA, Muzi M, Karp J, Mankoff DA, Kontos D. Functional 4-D clustering for characterizing intratumoral heterogeneity in dynamic imaging: evaluation in FDG PET as a prognostic biomarker for breast cancer. Eur J Nucl Med Mol Imaging. 2021;48:3990–4001.

76. Hotta M, Minamimoto R, Gohda Y, Miwa K, Otani K, Kiyomatsu T, Yano H. Prognostic value of ^{18}F-FDG PET/CT with texture analysis in patients with rectal cancer treated by surgery. Annal Nucl Med. 2021;35:843–52.

77. Cho H, Kim S, Jo K, Jeong YH, Kang WJ. Tumor glucose metabolism and its heterogeneity on F-18 FDG PET/CT provides better prognostication in nonmetastatic human papillomavirus-related oropharyngeal squamous cell cancer. Cancers. 2021;13:5538.

78. Nakajo M, Jinguji M, Nakabeppu Y, Nakajo M, Higashi R, Fukukura Y, Sasaki K, Uchikado Y, Natsugoe S, Yoshiura T. Texture analysis of ^{18}F-FDG PET/CT to predict tumour response and prognosis of patients with esophageal cancer treated by chemoradiotherapy. Eur J Nucl Med Mol Imaging. 2017;44(2):206–14.

79. Shrestha S, Higuchi T, Shirai K, Tokue A, Shrestha S, Saitoh JI, Hirasawa H, Ohno T, Nakano T, Tsushima Y. Prognostic significance of semi-quantitative FDG-PET parameters in stage I non-small cell lung cancer treated with carbon-ion radiotherapy. Eur J Nucl Med Mol Imaging. 2020;47(5):1220–7.

80. Gu B, Zhang J, Ma G, Song S, Shi L, Zhang Y, Yang Z. Establishment and validation of a nomogram with intratumoral heterogeneity derived from ^{18}F-FDG PET/CT for predicting individual conditional risk of 5-year recurrence before initial treatment of nasopharyngeal carcinoma. BMC Cancer. 2020;20(1):37.

81. Ma G, Gu B, Hu J, Kong L, Zhang J, Li Z, Xue Y, Lu J, Cao J, Cheng J, Zhang Y, Song S, Yang Z. Pretreatment ^{18}F-FDG uptake heterogeneity can predict treatment outcome of carbon ion radiotherapy in patients with locally recurrent nasopharyngeal carcinoma. Ann Nucl Med. 2021;35(7):834–42.

82. Schurink NW, van Kranen SR, Berbee M, van Elmpt W, Bakers FCH, Roberti S, van Griethuysen JJM, Min LA, Lahaye MJ, Maas M, Beets GL, Beets-Tan RGH, Lambregts DMJ. Studying local tumour heterogeneity on MRI and FDG-PET/CT to predict response to neoadjuvant chemoradiotherapy in rectal cancer. Eur Radiol. 2021;31(9):7031–8.

83. Arnett AL, Packard AT, Mara K, Mansfield AS, Wigle DA, Haddock MG, Park SS, Olivier KR, Garces YI, Merrell KW. FDG-PET parameters as predictors of pathologic response and nodal clearance in patients with stage III non-small cell lung cancer receiving neoadjuvant chemoradiation and surgery. Pract Radiat Oncol. 2017;7(6):e531–41.

84. Martens RM, Noij DP, Ali M, Koopman T, Marcus JT, Vergeer MR, de Vet H, de Jong MC, Leemans CR, Hoekstra OS, de Bree R, de Graaf P, Boellaard R, Castelijns JA. Functional imaging early during (chemo)radiotherapy for response prediction in head and neck squamous cell carcinoma; a systematic review. Oral Oncol. 2019;88:75–83.

85. Tang L, Wang XJ, Baba H, Giganti F. Gastric cancer and image-derived quantitative parameters: part 2-a critical review of DCE-MRI and ^{18}F-FDG PET/CT findings. Eur Radiol. 2020;30(1):247–60.

86. Ayati N, Sadeghi R, Kiamanesh Z, Lee ST, Zakavi SR, Scott AM. The value of ^{18}F-FDG PET/CT for predicting or monitoring immunotherapy response in patients with metastatic melanoma: a systematic review and meta-analysis. Eur J Nucl Med Mol Imaging. 2021;48(2):428–48.

87. Han S, Kim YI, Woo S, Kim TH, Ryu JS. Prognostic and predictive values of interim ^{18}F-FDG PET during neoadjuvant chemoradiotherapy for esophageal cancer: a systematic review and meta-analysis. Ann Nucl Med. 2021;35(4):447–57.

88. Han L, Wang Q, Zhao L, Feng X, Wang Y, Zou Y, Li Q. A systematic review and meta-analysis of the prognostic impact of pretreatment fluorodeoxyglucose positron emission tomography/computed tomography parameters in patients with locally advanced cervical cancer treated with concomitant chemoradiotherapy. Diagnostics (Basel). 2021;11(7):1258.

89. Jiang M, Zhang X, Chen Y, Chen P, Guo X, Ma L, Gao Q, Mei W, Zhang J, Zheng J. A review of the correlation between epidermal growth factor receptor mutation status and ^{18}F-FDG metabolic activity in non-small cell lung cancer. Front Oncol. 2022;20(12):780186.

90. Ito K, Kitajima K, Toriihara A, et al. ^{18}F-FDG PET/CT for monitoring anti-PD-1 therapy in patients with non-small cell lung cancer using SUV harmonization of results obtained with various types of PET/CT scanners used at different centers. Ann Nucl Med. 2021;35:1253–63.

91. Ayati N, Lee ST, Zakavi SR, et al. Response evaluation and survival prediction after PD-1 immunotherapy in patients with non-small cell lung cancer: comparison of assessment methods. J Nucl Med. 2021;62:926–33.

92. Johnson P, Federico M, Kirkwood A, Fosså A, Berkahn L, Carella A, d'Amore F, Enblad G, Franceschetto A, Fulham M, Luminari S, O'Doherty M, Patrick P, Roberts T, Sidra G, Stevens L, Smith P, Trotman J, Viney Z, Radford J, Barrington S. Adapted treatment guided by interim PET-CT scan in advanced Hodgkin's lymphoma. N Engl J Med. 2016;374(25):2419–29.

93. Duhrsen U, Muller S, Hertenstein B, et al. Positron emission tomography–guided therapy of aggressive non-Hodgkin lymphomas (PETAL): A Multicenter, Randomized Phase III Trial. J Clin Oncol. 2018;36(20):2024–34.

94. Cheson BD, Pfistner B, Juweid ME, Gascoyne RD, Specht L, Horning SJ, Coiffier B, Fisher RI, Hagenbeek A, Zucca E, et al. Revised response criteria for malignant lymphoma. J Clin Oncol. 2007;25:579–86.

95. Barrington SF, Mikhaeel NG, Kostakoglu L, Meignan M, Hutchings M, Müeller SP, Schwartz LH, Zucca E, Fisher RI, Trotman J, et al. Role of imaging in the staging and response assessment of lymphoma: consensus of the international conference on malignant lymphomas imaging working group. J Clin Oncol. 2014;32:3048–58.

96. Meignan M, Cottereau AS, Versari A, Chartier L, Dupuis J, Boussetta S, Grassi I, Casasnovas RO, Haioun C, Tilly H, et al. Baseline metabolic tumor volume predicts outcome in high-tumor-burden follicular lymphoma: a pooled analysis of three multicenter studies. J Clin Oncol. 2016;34:3618–26.

97. Toledano MN, Desbordes P, Banjar A, Gardin I, Vera P, Ruminy P, Jardin F, Tilly H, Becker S. Combination of baseline FDG PET/CT total metabolic tumour volume and gene expression profile have a robust predictive value in patients with diffuse

large B-cell lymphoma. Eur J Nuclear Med Mol Imaging. 2018;45:680–8.

98. Vercellino LZ, Cottereau AS, Casasnovas O, Tilly H, Feugier P, Chartier L, Fruchart C, Roulin L, Oberic L, Pica GM, et al. High total metabolic tumor volume at baseline predicts survival independent of response to therapy. Blood. 2020;135:1396–405.

99. Tamaki N, Kotani T, Nishimura M, Kaji T. Dynamic whole-body FDG-PET for oncology studies. Clinical Translational Imaging. 2022;10:249–58.

100. Sundaraiya S, Nangia S, Sirohi B, Patil S. Role of dynamic and parametric whole-body FDG PET/CT imaging in molecular characterization of primary breast cancer: a single institution experience. Nucl Med Commun. 2022;43(9):1015–25.

101. Sari H, Mingels C, Alberts I, Hu J, Buesser D, Shah V, Schepers R, Caluori P, Panin V, Conti M, Afshar-Oromieh A, Shi K, Eriksson L, Rominger A, Cumming P. First results on kinetic modelling and parametric imaging of dynamic $^{18}$F-FDG datasets from a long axial FOV PET scanner in oncological patients. Eur J Nucl Med Mol Imaging. 2022;49(6):1997–2009.

102. Lv W, Yang M, Zhong H, Wang X, Yang S, Bi L, Xian J, Pei X, He X, Wang Y, Lin Z, Cao Q, Jin H, Shan H. Application of dynamic $^{18}$F-FDG PET/CT for distinguishing intrapulmonary metastases from synchronous multiple primary lung cancer. Mol Imaging. 2022;30(2022):8081299.

103. Wang D, Zhang X, Liu H, Qiu B, Liu S, Zheng C, Fu J, Mo Y, Chen N, Zhou R, Chu C, Liu F, Guo J, Zhou Y, Zhou Y, Fan W, Liu H. Assessing dynamic metabolic heterogeneity in non-small cell lung cancer patients via ultra-high sensitivity total-body [$^{18}$F]FDG PET/CT imaging: quantitative analysis of [$^{18}$F]FDG uptake in primary tumors and metastatic lymph nodes. Eur J Nucl Med Mol Imaging. 2022. https://doi.org/10.1007/s00259-022-05904-8.

104. Marin A, Murchison JT, Skwarski KM, Tavares AAS, Fletcher A, Wallace WA, Salapura V, van Beek EJR, Mirsadraee S. Can dynamic imaging, using $^{18}$F-FDG PET/CT and CT perfusion differentiate between benign and malignant pulmonary nodules? Radiol Oncol. 2021;55(3):259–67.

105. Sundaraiya S, Raja T, Nangia S, Sirohi B, Patil S. Role of dynamic and parametric whole-body FDG PET/CT imaging in molecular characterization of primary breast cancer: a single institution experience. Nucl Med Commun. 2022;43(9):1015–25.

106. Hsu DFC, Ilan E, Peterson WT, Uribe J, Lubberink M, Levin CS. Studies of a next-generation silicon-photomultiplier–based time-of-flight PET/CT system. J Nucl Med. 2017;58:1511–8.

107. van Sluis J, De Jong J, Schaar J, et al. Performance characteristics of the digital biograph vision PET/CT system. J Nucl Med. 2019;60:1031–6.

108. Rausch I, Ruiz A, Valverde-Pascual I, Cal-González J, Beyer T, Carrio I. Performance evaluation of the Philips Vereos PET/CT system according to the NEMA NU2-2012 standard. J Nucl Med. 2019;60:561–7.

109. Beyer T, Bidaut L, Dickson J, Kachelriess M, Kiessling F, Leitgeb R, Ma J, Shiyam Sundar LK, Theek B, Mawlawi O. What scans we will read: imaging instrumentation trends in clinical oncology. Cancer Imaging. 2020;20(1):38.

110. Zaidi H, Alavi A, Naqa IE. Novel Quantitative PET techniques for clinical decision support in oncology. Semin Nucl Med. 2018;48(6):548–64.

111. Seifert R, Kersting D, Rischpler C, Opitz M, Kirchner J, Pabst KM, Mavroeidi IA, Laschinsky C, Grueneisen J, Schaarschmidt B, Catalano OA, Herrmann K, Umutlu L. Clinical use of PET/MR in oncology: an update. Semin Nucl Med. 2022;52(3):356–64.

112. Nakamoto Y, Kitajima K, Toriihara A, Nakajo M, Hirata K. Recent topics of the clinical utility of PET/MRI in oncology and neuroscience. Ann Nucl Med. 2022;36(9):798–803.